Received: 20 July 2022 | Revised: 6 December 2022 | Accepted: 16 December 2022

DOI: 10.1096/fj.202201157RR

THE FASEB JOURNAL

RESEARCH ARTICLE

Targeting SARS-CoV-2 by synthetic dual-acting thiol compounds that inhibit Spike/ACE2 interaction and viral protein production

Alessandra Fraternale[1] | Marta De Angelis[2] | Riccardo De Santis[3] | Donatella Amatore[3] | Sofia Masini[1] | Francesca Monittola[1] | Michele Menotta[1] | Federica Biancucci[1] | Francesca Bartoccini[1] | Michele Retini[1] | Valentina Fiori[4] | Raoul Fioravanti[5] | Fabio Magurano[5] | Laura Chiarantini[1] | Florigio Lista[3] | Giovanni Piersanti[1] | Anna T. Palamara[2,5] | Lucia Nencioni[2] | Mauro Magnani[1] | Rita Crinelli[1]

[1]Department of Biomolecular Sciences, University of Urbino Carlo Bo, Urbino, Italy

[2]Department of Public Health and Infectious Diseases, Laboratory Affiliated to Istituto Pasteur Italia-Fondazione Cenci Bolognetti, Sapienza University of Rome, Rome, Italy

[3]Scientific Department, Army Medical Center, Rome, Italy

[4]DIATHEVA SRL, Cartoceto, Italy

[5]Department of Infectious Disease, Istituto Superiore di Sanità, Rome, Italy

Correspondence
Alessandra Fraternale, Department of Biomolecular Sciences, University of Urbino Carlo Bo, Via Saffi, 2 61029 Urbino, Italy.
Email: alessandra.fraternale@uniurb.it

Funding information
Ministero dell'Università e della Ricerca (MUR), Grant/Award Number: MUR PRIN 2020KSY3KL and MUR PRIN 2020AEX4TA; Sapienza Università di Roma (Sapienza University of Rome), Grant/Award

Abstract

The SARS-CoV-2 life cycle is strictly dependent on the environmental redox state that influences both virus entry and replication. A reducing environment impairs the binding of the spike protein (S) to the angiotensin-converting enzyme 2 receptor (ACE2), while a highly oxidizing environment is thought to favor S interaction with ACE2. Moreover, SARS-CoV-2 interferes with redox homeostasis in infected cells to promote the oxidative folding of its own proteins. Here we demonstrate that synthetic low molecular weight (LMW) monothiol and dithiol compounds induce a redox switch in the S protein receptor binding domain (RBD) toward a more reduced state. Reactive cysteine residue profiling revealed that all the disulfides present in RBD are targets of the thiol compounds. The reduction of disulfides in RBD decreases the binding to ACE2 in a cell-free system as demonstrated by enzyme-linked immunosorbent and surface plasmon resonance (SPR) assays. Moreover, LMW thiols interfere with protein oxidative folding and the production of newly synthesized polypeptides in HEK293 cells expressing the S1 and RBD domain, respectively. Based on these results, we hypothesize that these thiol compounds impair both the binding of S protein to its cellular receptor during the early stage of viral infection, as well as viral protein folding/maturation and thus the formation of new viral mature particles. Indeed, all the tested molecules, although at different concentrations, efficiently inhibit both SARS-CoV-2

Abbreviations: ACE2, angiotensin-converting enzyme 2 receptor; DTT, dithiothreitol; GSH, reduced glutathione; HRP, horseradish peroxidasechain; IAM, 2-Iodacetamide; LMW, low molecular weight; MEA, cysteamine; NAC, N-acetylcysteine; PEGmal, polyethylene glycol maleimide; RDB, receptor binding domain; RT, room temperature; S, spike protein; SPR, surface plasmon resonance.

Correction added on February 16, 2023, after first Online publication: Co-author name "Romano F. Lista" changed to "Florigio Lista".

Number: RM120172B6D0AD25 and RP12117A62FD5A1A; Università degli Studi di Urbino Carlo Bo (UNIURB), Grant/Award Number: DISB_CRINELLI_PROG_SIC_ALIMENTARE

entry and replication in Vero E6 cells. LMW thiols may represent innovative anti-SARS-CoV-2 therapeutics acting directly on viral targets and indirectly by inhibiting cellular functions mandatory for viral replication.

KEYWORDS

disulfide bonds, oxidative folding, respiratory viruses, SARS-CoV-2, spike protein, thiol molecules

1 | INTRODUCTION

The environmental redox state is an important factor for enveloped viruses' life cycle. The thiol–disulfide balance plays an important role in receptor recognition by the SARS-CoV-2 spike (S) protein. Given that a correct protein conformation is required for protein function and that disulfide bonds are often crucial both for structural stability and conformational changes, it is not surprising that the reduction of the disulfides into sulfhydryl groups in the receptor binding domain (RBD) seriously impairs the binding to ACE2.[1,2] Thus, manipulation of the redox status of the cysteine-rich glycoproteins in the virus envelope can influence viral cell entry. Cleavage of disulfide bonds by thiol-reducing compounds can efficiently weaken viral binding and prevent SARS-CoV-2 infection.[3–6] Maturation of spike glycoprotein requires the formation of disulfide bonds in the endoplasmic reticulum (ER) that are necessary for its folding and function.[7] A correct formation of viral disulfides is particularly important in the RBD region that directly participates in binding to the host receptor and contributes to the general mechanical stability of the homotrimeric spike.[8] ER is in an oxidizing environment necessary for oxidative protein folding[9] and respiratory viruses modify the intracellular redox state toward a pro-oxidant condition to benefit viral replication.[10,11] In particular, SARS-CoV-2 infection modifies the levels and metabolism of reduced glutathione (GSH) in the host cell, with consequent loss of intracellular redox homeostasis.[12] These premises lead to hypothesize that SARS-CoV-2 infectivity may be affected not only by the extracellular disulfide thiol balance[1–6] but also by the intracellular redox systems.[12] An intracellular reductive shift induced by thiol-based drugs may lead to impairment of viral protein folding and secretion. In previous works, including ours, it has been shown the GSH-replenishing and antiviral activities of low molecular weight (LMW) thiols.[13–16] The LMW thiols previously studied and also included in this investigation were the n-butanoyl derivative of GSH (C4-GSH) and I-152, a conjugate of N-acetylcysteine (NAC) and S-acetyl-cysteamine (SMEA). C4-GSH was designed and synthesized with the aim to increase the stability of GSH in circulation and to overcome the problems of cell permeability of the tripeptide.[17] I-152 was originally synthesized as an anti-HIV compound able to release NAC and cysteamine (MEA) to boost intracellular GSH content.[13–18] Afterwards, C4-GSH was demonstrated to interfere with haemagglutinin folding and maturation resulting in inhibition of influenza virus replication[19] and I-152 impaired immunoglobulin G folding and secretion in a murine model of hypergammaglobulinemia.[14] The results of the present study demonstrate that the thiol molecules weaken the binding RBD/ACE2 by reducing the four disulfide pairs situated in the RBD and affect protein folding/secretion in cells expressing recombinant RBD/S1 protein domains. In agreement with these findings, pretreatment of SARS-CoV-2 particles with the molecules strongly inhibited virus entry. Moreover, a strong inhibition of intracellular virus replication was found when host-infected cells were incubated with the molecules, indicating that the intracellular phase of the SARS-CoV-2 life cycle was inhibited as well. In conclusion, thiol-based drugs represent new antiviral therapies targeting viral components, i.e., RBD, and host factor activity likely involved in virus protein folding/maturation.

2 | MATERIALS AND METHODS

2.1 | Materials

Cysteamine (MEA), dithiothreitol (DTT), diamide, and methoxy polyethylene glycol 5000 maleimide (mPEG-mal5000) were purchased from Merck KGaA (Darmstadt, Germany). C4-GSH was synthesized by Gluos Srl (Urbino, Italy).[20]

I-152 and I-152SdAc were synthesized as described previously resulting in comparable yields and identical NMR spectra.[13,21]

Anti S1 antibody, recombinant SARS-CoV-2 Spike protein RBD domain (aa 304-526) as well as HEK293 cells stably expressing the Spike S1 subunit (with D614G mutation) or the RBD domain were a generous gift of Diatheva SRL (Cartoceto, Italy). The proteins were engineered to carry an N-terminal signal peptide for secretion and a C-terminal His tag for purification.

SARS-CoV-2 Receptor Binding Domain (RBD, GenBank: QHD43416, Sigma-Aldrich, St. Louis, USA)

was used in SPR and spectrometry studies. Recombinant Human Angiotensin-converting Enzyme 2 (ACE2, Acc.N: Q9BYF1, RayBiotech, Peachtree Corners, USA); Sensor chip CM5, HBS-EP+ buffer (10 mM HEPES pH 7.4; 150 mM NaCl; 3 mM EDTA; 0.05% P20) and Acetate Buffer pH 5.5 were purchased from Cytiva (Cytiva life sciences, Marlborough, USA).

2.2 | In vitro incubation of recombinant SARS-CoV-2 Spike protein RBD domain with thiol molecules

The recombinant SARS-CoV-2 Spike protein RBD (1–5 μg) domain was incubated at 37°C with the LMW thiol molecules in phosphate-buffered saline (PBS) for 1 h. At the end of the incubation, a 5-fold molar excess of Iodoacetamide was added to the mixture to inactivate the molecules and alkylate protein -SH groups, and the samples were further incubated for 1 h at room temperature in the dark. The samples were then used for western immunoblotting or mass spectrometry-based analyses.

For SPR measurements, RBD and thiols (final concentration 2 mM) were incubated in HBS-EP+ buffer at 37°C for 1 h. To limit the effects of the thiols on the measurements, after incubation, thiol concentration was reduced by repeated steps of dilution and ultrafiltration with Amicon Ultra 0.5 (3 kDa MWCO, Millipore, Merck Group, Darmstadt, Germany) and RBD final concentration adjusted to 1×10^{-6}M (stock solution).

2.3 | Western immunoblotting analysis of recombinant SARS-CoV-2 Spike protein RBD domain after incubation with the thiol molecules

The samples incubated as described above were diluted in non-reducing Sodium Dodecyl Sulphate (SDS) sample buffer, heated at 100°C, and resolved by SDS-PAGE. Fully reduced [R] and non-reduced [NR] RBD used as a reference were obtained by diluting the protein in SDS sample buffer containing or not 4% (v/v) β-mercaptoethanol, respectively. For detection, the protein was blotted onto PVDF membranes and immune-stained with anti 6X His tag rabbit polyclonal antibody (OriGene Technologies Inc, Rockville, MD, USA). Detection was performed using a goat anti-rabbit horseradish peroxidase (HRP)-conjugated secondary antibody (Bio-Rad, Hercules, CA, USA) and the enhanced chemiluminescence detection kit WesternBright ECL (Advasta, San Jose, CA, USA). Immunoreactive bands were visualized in a ChemiDoc MP Imaging System (Bio-Rad).

2.4 | Mass spectrometry-based analysis

LC–MS/MS was performed by the Orbitrap Exploris™ 240 Mass Spectrometer (Thermo Fisher Scientific) coupled with the Ultimate 3000 LC system. After RBD treatment, samples were digested by Trypsin/LysC and the obtained peptides were BCA assayed. Ten ng of each sample was loaded onto the trap column AcclaimTM PepMapTM 100 C18 75 μm × 2 cm LC Columns (Thermo Scientific™; Waltham, MA, USA) at a flow rate of 10 μl/min and were then separated with a Thermo RSLC Ultimate 3000 (Thermo Scientific™; Waltham, MA, USA) on a Thermo Easy-SprayTM PepMap RSLC C18 2 μm, 100 Å, 75 μm × 15 cm column (Thermo Scientific™; Waltham, MA, USA) with a step gradient of 4%–60% solvent B (0.1% FA in 80% ACN) from 3–45 min and of 60%–90% solvent B for 45–50 min at 300 nL/min and 35°C, resulting in a 60 min total run time.

MS data were acquired using a data-dependent Top20 method dynamically choosing the most abundant precursor ions from the survey scan (300–1500 Th) for HCD fragmentation. For MS1orbitrap resolution was set to 120.000 (at m/z 200), target automatic gain control (AGC) values of 3×10^6, and auto maximum injection times. For MS2 orbitrap resolution was set to 60.000 (at m/z 200), target automatic gain control (AGC) values of 7.5×10^4, and 40 ms of maximum injection times. Fragmentation was performed with a normalized collision energy of 30. Charge survey (2–6) and dynamic exclusion options (mass tolerance 10 ppm) were employed.

2.5 | Spike/ACE2 interaction inhibition assay

Inhibition of SARS-CoV-2 spike and ACE2 interaction by thiol molecules was tested using the SARS-CoV-2 Spike-ACE2 interaction Inhibitor Screening Assay kit from Cayman Chemical (MI, USA). To evaluate whether the LMW thiols could disrupt the native form of S1 RBD, the protocol, was slightly modified: the recombinant SARS-CoV-2 spike S1 RBD bound to the pre-coated plate, was incubated with LMW thiols at 37°C for 1 h, and after several washes, the His-tagged ACE2 protein was added. All the remaining procedures were conducted as indicated by the manufacturer.

2.6 | Surface plasmon resonance assay

Kinetics studies were performed on a Biacore X100 (Cytiva). S protein (acc. #YP_009724390.1, R&D Systems, Biotechne, MSP, USA) was immobilized on a CM5 sensor

chip by the amine coupling method by using Acetate pH 5.0 and a final protein concentration of 50 µg/ml as described in manufacturer instructions. HBS-EP+ (10 mM HEPES buffer pH 7.4, 150 mM NaCl, 3 mM EDTA, 0.05% surfactant P20) was used as running and dilution buffer. Serial dilutions of the analyte (ACE2) were injected at 25°C with a flow rate of 30 µl/min while the RBD solution concentration (treated with the thiol molecules or untreated) was kept at 25 nM. The surface was regenerated between samples with a 70% ethylene glycol solution. All data were zero adjusted and the reference (blank) was subtracted. The quality of the fitted results was evaluated by the χ^2 parameter. The inhibition of ACE2 binding to RBD was calculated according to the equation:

$$\text{ACE2 inhibition}\,(\%) = \frac{K_{\text{RBDi}} - K_0}{K_{\text{RBD}} - K_0} \bullet 100$$

where K_{RBDi}, K_{RBD}, and K_0 represent the dissociation constants of the interaction ACE2-S protein measured in the presence of RBD pre-treated with the molecules, the functional RBD or the ACE2 alone, respectively, and the overall reaction is depicted below:

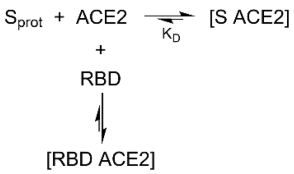

The interaction between the S protein and ACE2 was assessed in the conditions described above by injections of ACE2 without RBD. The reported values (Figure S1 and Table S1) are consistent with the manufacturer and the kinetics and thermodynamics constants for the ACE2-S protein interaction present in the literature.[22]

2.7 | Cell culture

HEK293 and Vero E6 cells were cultured in DMEM and MEM medium, respectively, supplemented with 10% (v/v) FBS, 2 mM glutamine, 100 µg/ml streptomycin, and 100 µg/ml penicillin.

2.8 | Analysis of RBD protein production/secretion in HEK293 cells after incubation with the thiol molecules

HEK293 cells expressing SARS-CoV-2 RBD recombinant protein were seeded at 120.000 cells/well in 24 well plates and after 2 days treated with different molecule concentrations for 24 h. Control cells received only fresh medium. After incubation, the medium was collected and centrifuged to remove any detached cells. The supernatant was transferred into a new tube while the pellet was washed with PBS and pooled with the cell lysate. Cells were lysed directly on the dish by adding 100 µl of SDS-lysis buffer (50 mM Tris–HCl, pH 7.8, 0.25 M sucrose, 2% (w/v) SDS, 10 mM N-ethylmaleimide (NEM)), supplemented with protease inhibitors (Complete, Roche, Basel, Switzerland). An aliquot of the culture medium (supernatant) and the cell lysate was analyzed by western immunoblotting using an anti-His tag antibody, as described above. Quantification of the immunoreactive bands was performed with the Image Lab software (Bio-Rad, Hercules, CA, USA). β-actin was stained as a loading control (Cell Signaling Technologies, Danvers, MA, USA).

2.9 | Polyethylene glycol maleimide (PEGmal) alkylation of sulfhydryl groups

HEK293 cells expressing SARS-CoV-2 S1 recombinant protein were treated with the molecules for 4 h. In control dishes, cells were incubated for 30 min with either 5 mM diamide to fully oxidize or 5 mM DTT to fully reduce S1. As control of the pegylation assay, untreated cells were incubated with 20 mM NEM in PBS for 20 min on ice. Cells were then washed in cold PBS and lysed in 10% (v/v) trichloroacetic acid (TCA) and 50% (v/v) acetone. After centrifugation, the pellet was washed three times in 80% (v/v) acetone, dried, and solubilized in a buffer consisting of 0.1 M Tris–HCl, pH 6.8, 8 M urea, 5 mM mPEGmal5000 and 1 mM ethylenediaminetetraacetic acid, adjusted to pH 7.0. The lysate was incubated for 2 h at room temperature in the dark and the reaction was stopped by adding 0.1 M DTT. Protein concentration was determined by the Bradford assay using BSA as standard. Ten µg of proteins were resolved on 6.5% (v/v) polyacrylamide gel and immunoblotted as described above using an anti-S1 monoclonal antibody.

2.10 | Glutathione and thiol species determination in HEK293 cells

HEK293 cells expressing SARS-CoV-2 RBD recombinant protein were seeded at 400.000 cells/well in 6 well plates and after 3 days treated with different molecule concentrations for 2 h. Thiol content was assayed as previously described.[23] Briefly, after treatment, cells were lysed with a buffer consisting of 0.1% (v/v) Triton X-100, 0.1 M Na_2HPO_4, 5 mM EDTA, pH 7.5. Then, 0.1 N HCl and precipitating solution (100 ml containing 1.67 g of glacial metaphosphoric acid, 0.2 g of disodium EDTA,

and 30 g of NaCl) were added. After centrifugation, the pellet was dissolved in 0.1 M NaOH and protein concentration was determined by the Bradford assay; the thiol species were determined in the supernatant by high-performance liquid chromatography (HPLC) method, validated according to USA and European standards. The method was based on separation coupled with ultraviolet detection and pre-column derivatization with 5,5′-dithiobis-(2-nitrobenzoic acid) (DTNB) as previously described.[24]

2.11 | Cytotoxicity assay

The cytotoxicity of LMW thiols was evaluated in Vero E6 cells by trypan blue exclusion. The data were used to calculate the CC50 (Cytotoxic concentration of the molecule that causes death to 50% of viable cells) value.

2.12 | Anti-viral activity

Virus. SARS-CoV-2 (hCoV-19/Italy/CDG1/2020/EPI_ISL_412973), isolated from a nasopharyngeal swab by the Department of Infectious Diseases, National Institute of Health Rome, Italy was propagated in Vero E6 cells to produce viral working stocks. The concentration of infectious virus was determined by plaque-forming titer assay. All the experiments with SARS-CoV-2 were performed in the Biological Safety Level 3 (BSL-3) laboratory of the Scientific Department, Army Medical Center, Rome, Italy.

Viral-entry inhibition assay. Two different protocols were performed. In the first one, SARS-CoV-2 (0.01 m.o.i.) was incubated with MEM containing the molecules for 1 h at 37°C in a 5% CO_2 incubator. Then, the mixtures were used to infect cells monolayer for 1 h at 37°C. After viral adsorption, the inoculum was removed, and a plaque assay was performed.

In the second protocol, it was evaluated the amount of infective viral particles released in the supernatants of the cells infected as above. Briefly, after 1 h incubation with the mixture (thiol molecule+virus), the medium was removed and replaced with fresh medium supplemented with 2% FBS and cells were maintained in a 5% CO_2 incubator for the following 24 h. Then, supernatants were collected and used to infect cells monolayer for 1 h at 37°C. After viral adsorption, the inoculum was removed, and a plaque assay was performed. Untreated SARS-CoV-2 was used as a positive control of viral infection in both protocols.

Post-infection treatment assay. Vero E6 cells seeded in a 24-well plate were infected for 1 h at 37°C with SARS-CoV-2 (0.01 m.o.i.); after 1 h incubation, the medium was removed and replaced with fresh medium containing the thiol molecules, supplemented with 2% FBS. After 24 h, the supernatants were collected and used to infect cells monolayer for 1 h at 37°C. After the viral adsorption period, the inoculum was removed, and a plaque assay was performed. Infected-untreated cells were used as a positive control of viral infection.

2.13 | Plaque assay

Vero E6 cells were overlaid with a mixture of MEM (no glutamine, no phenol-red-GIBCO), 1.5% Tragacanth (SIGMA), $NaHCO_3$ 7% (Gibco), L-glutamine 1X (Gibco), MEM NEAA 1x (Gibco), 0.02 M Hepes (Euroclone), DMSO (Sigma-Aldrich) and 2% FBS (final concentration). To calculate PFU, 5 days post-infection the mixture was removed carefully, plates were washed with saline solution, and stained with 1% crystal violet for 20 min. The plaque reduction ratio was calculated as $(100 - N/N_0 \times 100)$ where N is the PFU count of the treated sample, and N_0 is the PFU count of the control sample.

The plaque assay was also used to determine the concentration of molecule that inhibits 50% of plaques in each well (IC50).

2.14 | Protein extraction and western immunoblotting analysis of viral proteins

Vero E6 cells were lysed with RIPA buffer [20 mM Tris–HCl pH 8.0, 150 mM NaCl, 1% (v/v) Triton X-100, 0.5% (w/v) sodium dodecyl sulfate (SDS) and 1% (w/v) sodium deoxycholate] supplemented with phenylmethylsulfonyl fluoride, protease and phosphatase inhibitor cocktails (Sigma-Aldrich, Milan, Italy) in BSL-3 facilities. Cell lysates were centrifuged (13 000 rpm, 30 min, 4°C) and the supernatants were diluted in SDS sample buffer containing DL-Dithiothreitol (DTT 0.1 M). The total extract was analyzed by SDS-PAGE followed by western immunoblotting. Membranes were stained with anti-Spike (GeneTex Cat No. GTX632604) or anti Nucleocapsid (Rockland Cat. No. 200-401-A50) antibodies and then incubated with HRP-linked anti-mouse or anti-rabbit (Jackson ImmunoResearch, Newmarket, UK) antibodies as secondary antibodies. The membranes were developed using Clarity Western ECL substrate (Bio-Rad, Hercules, CA, USA).

2.15 | Statistical analysis

Statistical analysis was performed by GraphPad Prism™ 6.0 software (GraphPad Software Inc., San Diego, California, USA) using a one-way Anova test. A p-value $<.05$ was considered statistically significant. For MS data, statistical evaluation

was performed by Friedman test followed by Dunn's multiple comparisons test (Dunn correction, Alpha .05).

3 | RESULTS

3.1 | Thiol molecules cause disulfide bond reduction in recombinant SARS-CoV-2 Spike protein RBD domain and inhibit RBD/ACE2 interaction

The thiol molecules investigated for their ability to disrupt disulfide bonds of the Spike protein were the monothiols C4-GSH and I-152; moreover, the S-deacetylated dithiol derivative of I-152 (I-152SdAc)[21] was added to our analyses based on the virucidal activity results of mono and dithiol molecules recently reported[5] (Figure 1A). To evaluate the capacity of our thiols to interfere with the receptor-binding processing of the Spike protein, we chose to perform our investigations by using the RBD domain instead of the entire trimeric Spike considering the critical role of the four S-S bridges of the RBD in the Spike RBD–ACE2 interaction before fusion process.[6] Most studies previously conducted on the activity and mechanism of action of thiol-based reducing agents against SARS-CoV-2 recognition and entry were based on RBD/ACE2 recognition-based assays.[5,6,25]

After incubation of the recombinant RBD protein domain with different molecule concentrations, samples were subjected to non-reducing denaturing polyacrylamide gel electrophoresis (PAGE) where proteins with S-S bonds maintain a more compact conformation than the reduced protein and thus run faster.[26] RBD detection was performed on blotted gels with an anti-His tag antibody. Under these conditions, an evident mobility shift of the RBD protein band, from the non-reduced [NR] toward the reduced [R] form was observed as the molecule concentration increased (Figure 1B). In addition, since the NR form was less immunoreactive compared to the reduced one, probably due to epitope masking, reduction of S-S bonds was also observed as changes in the intensity of the chemiluminescent signal which becomes more intense as disulfides are progressively broken and the His tag becomes more accessible to the antibody. Results of Figure 1B show that all the tested molecules, although

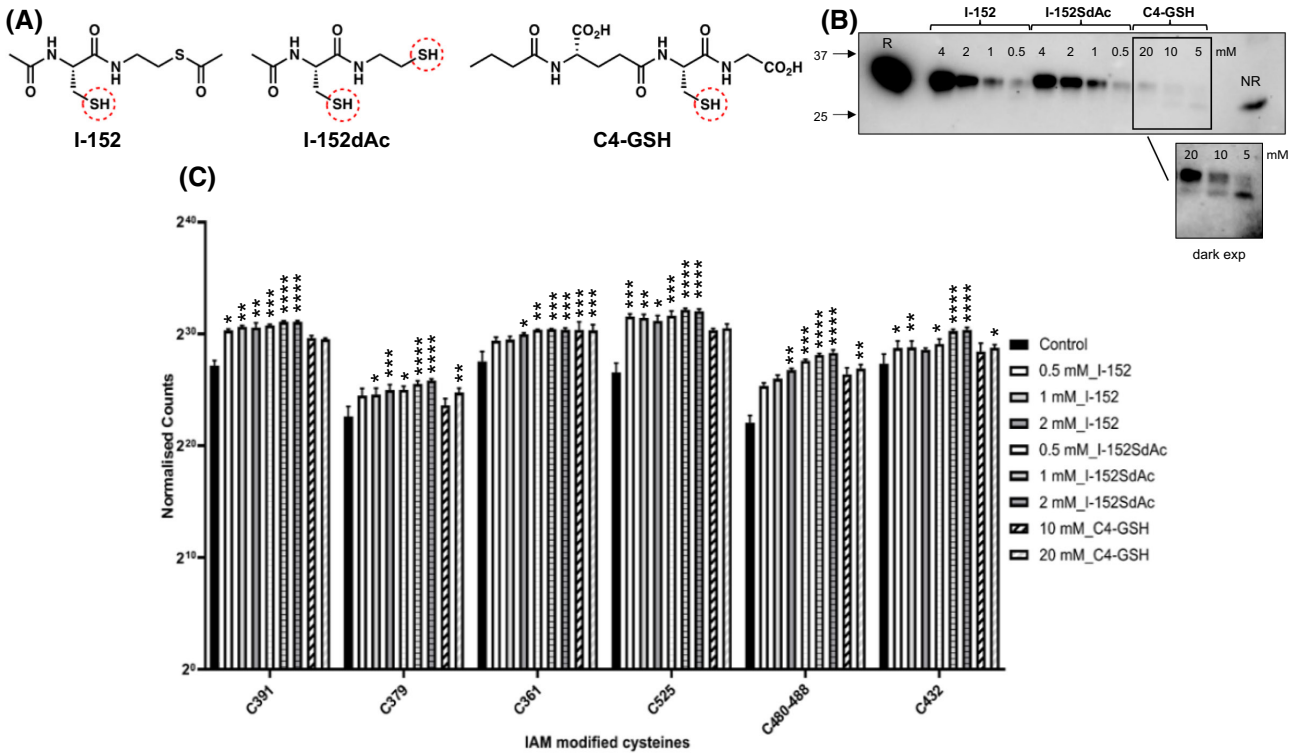

FIGURE 1 Modification of the RBD domain conformation by thiol molecules. (A) Chemical structure of I-152, I-152SdAc and C4-GSH (B) Western immunoblotting analysis of recombinant spike protein RBD domain after incubation with the molecules and separation by non-reducing SDS-PAGE. An equal amount of protein was incubated with different molecule concentrations. As reference fully reduced (R) and non-reduced (NR) protein was run in parallel. A double amount of NR protein was loaded on the gel to increase signal intensity. On the left, the position of molecular weight standards (kDa) is indicated by arrows. (C) Normalized counts from MS data showing the amounts of IAM-modified cysteines by thiol molecules. The annexed table reports the statistical comparisons among samples for each residue. I-152SdAc showed the greater impact. ****$p < 10^{-4}$; ***$p < 10^{-3}$; **$p < 10^{-2}$; *$p < 5 \times 10^{-2}$.

to a different extent, were able to change the electrophoretic mobility of the protein. The most evident mobility shifts and increase in signal intensity were observed with I-152 and I-152SdAc, while C4-GSH, had modest effects that could be appreciated only after prolonged exposure of the blot (Figure 1B, dark exposure).

To identify the disulfides targeted by thiol molecules, peptide mapping analysis by mass spectrometry was performed. For this purpose, the 2-Iodacetamide (IAM) modified cysteines, in controls and after treatments, were studied. In Figure 1C the amounts of IAM alkylated discovered cysteines, are reported. Compared to the control condition, the I-152 and I-152SdAc-treated samples showed more alkylated residues compared to the C4-GSH ones (Dunn's test, remarkably the C4-GSH condition was examined 10-fold more concentrated). This evidence supports the concept that the proposed thiol molecules caused disulfide bond reduction in the RBD protein.

To test if the perturbation in the RBD redox assessment induced by the LMW thiols could reduce the affinity of the protein for ACE2, the RBD/ACE2 interaction was quantified by a SARS-CoV-2 Spike-ACE2 interaction inhibitor screening assay. We found that all three tested molecules inhibited RBD binding to ACE2 in a dose-dependent manner, but their potency varied according to the number of the thiol groups present in the molecule (Figure 2A). In fact, the most marked binding inhibition was found with I-152SdAc and I-152 followed by C4-GSH, which was tested at higher doses in agreement with the results shown in Figure 1. Half maximal inhibitory concentration (IC50) values calculated for the thiol molecules were 2.6, 3.9, and 9.7 mM for I-152SdAc, I-152, and C4-GSH, respectively. Interaction between ACE2 and RBD pre-incubated with the thiol molecules, which had shown the strongest activity in the previous tests (i.e., I-152 and I-152SdAc), was further characterized by SPR measurements. The binding activity of the RBD (in solution, pre-incubated or not with the thiol molecules, at 2 mM concentration) was assessed by measuring the interaction of ACE2, the analyte, with the functional S protein immobilized on the chip. The SPR sensorgrams show a decrease in the curvature, which is indicative of the interaction phase, moving from the fully functional RBD (Untreated) toward the I-152SdAc-reduced RBD (I-152SdAc) (Figure 2B). The apparent KD measurements follow the same trend, with values of 3.53×10^{-7} M, 1.33×10^{-7} M, and 5.45×10^{-8} M for RBD, I-152-treated RBD, and I-152SdAc-treated RBD, respectively. The calculated decrease in the binding activity of

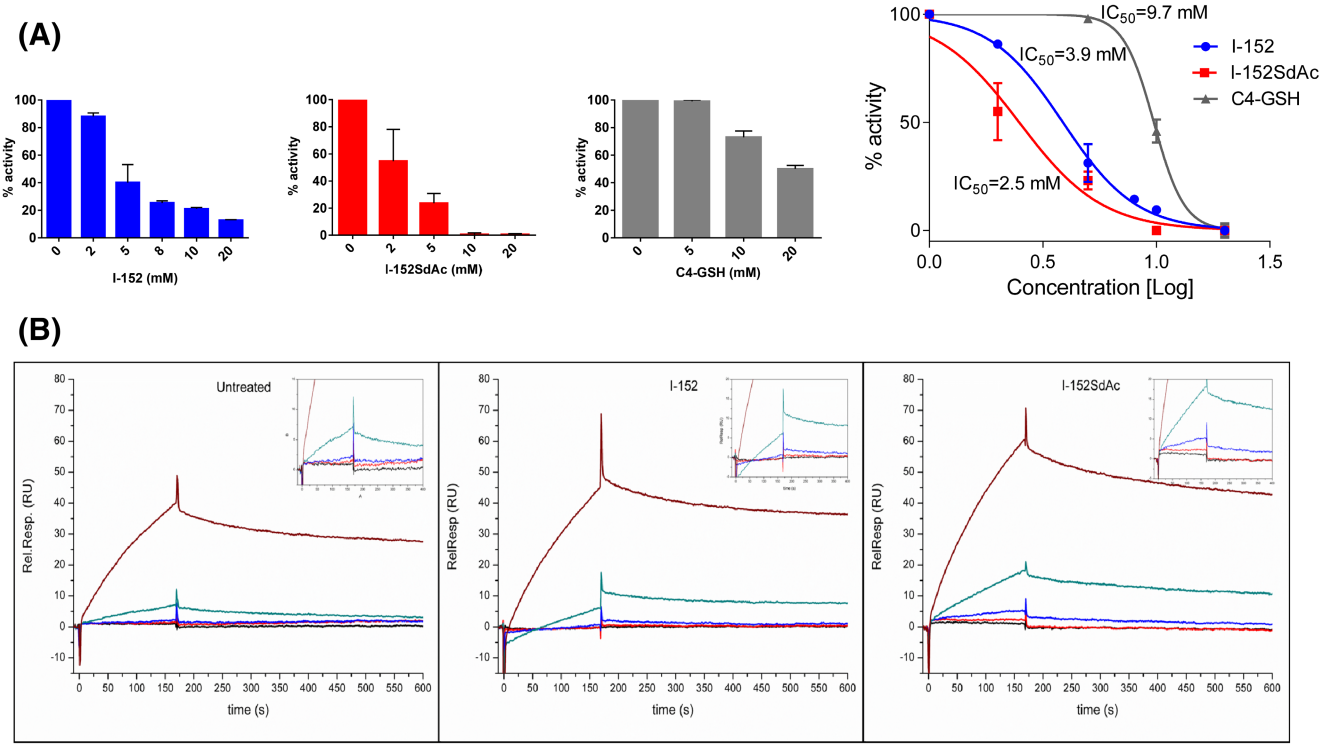

FIGURE 2 Impairment of RBD/ACE2 interaction by thiol molecules. (A) RBD/ACE2 binding activity evaluated by an ELISA. Data are represented as percent activity as a function of thiol molecule concentration. Data are the mean of duplicate measurements from three independent experiments ± standard deviation. The IC50 value was determined and graphed by GraphPad Prism 6.0. (B) SPR sensorgrams of S protein-ACE2 interaction with RBD in solution. Sensorgram of the multicycle interaction between ACE2 and untreated RBD (left); I-152-treated RBD (middle) and I-152dAc-treated RBD (right). RBD concentration was kept at 25 nM while ACE2 concentrations are 100 nM (wine), 25 nM (dark cyan), 5 nM (blue), 1 nM (red), and 0.2 nM (black). Experiments were repeated three times.

ACE2 to I-152-treated RBD was about 63% compared to that measured in the presence of untreated RBD, but the highest inhibition was measured with I-152SdAc (85%).

3.2 | Thiol molecules inhibit SARS-CoV-2 entry and replication in Vero E6 cells

Based on the results obtained by cell-free experimental models (Figures 1 and 2), SARS-CoV-2 suspensions, pre-incubated with I-152, I-152SdAc and MEA (2 mM) or C4-GSH (20 mM), (thiol molecule+virus), were used to evaluate the virucidal activity of the molecules. In these tests, MEA effectiveness was also investigated since it is a metabolite of I-152 and I-152SdAc within cells and it has been previously described as an effective SARS-CoV-2 entry inhibitor.[27] Moreover, MEA is an approved drug, being the specific targeted therapy for cystinosis treatment.[28,29]

All the reducing agents were able to significantly impair the infectivity of SARS-CoV-2. Pre-incubation of the virus with I-152 and I-152SdAc caused a decrease in the number of plaques by about 86% and 95% respectively, while about 80% reduction was obtained with MEA and C4-GSH, demonstrating that these reducing molecules strongly impair virus entry (Figure 3A). The antiviral effect was confirmed by the western blot analysis of the viral proteins, Spike (S) and Nucleocapsid (N), in lysates obtained from the cells infected with the virus pre-incubated with the thiol molecules (Figure 3B). We can observe that the thiol compounds reduced S protein to undetectable levels, and N protein almost disappeared with I-152SdAc treatment while it was strongly reduced by I-152 and, to a less extent, by MEA and C4-GSH. Calculation of the amount of infective viral particles released in the supernatant of the infected cells nearly confirmed the results reported in the previous test (Figure 3C). In agreement with the results reported in Figures 1 and 2, the most effective compound was I-152SdAc indicating that the number of thiol groups of the molecules may affect the potency of the thiols to impair the viral entry into the cell.

In our previous works we have demonstrated that one mechanism by which the thiol molecules could inhibit viral infection was by interfering with protein maturation/secretion.[14,19] Hence, we explored whether the thiol molecules also inhibited intracellular SARS-CoV-2 life cycle's step. To this aim, Vero E6 cells were infected with SARS-CoV-2 and the thiol molecules were added for the following 24 h (I-152, MEA, I-152SdAC at the dose of 0.25 mM and C4-GSH at the dose of 10 mM). The plaque assay showed that all the LMW thiols impaired viral replication, although with different efficiencies (Figure 3D). Treatment with I-152 and I-152SdAc led to over 90% reduction in virus production while in the case of MEA and C4-GSH the inhibition was by about 50% (Figure 3D).

Similarly, viral protein expression analysis revealed that thiols were able to interfere with viral replication and confirmed the highest inhibition mediated by I-152SdAc and I-152 (Figure 3E). Thus, the inhibitory effect of I-152 and I-152SdAc was further explored in Vero E6 cells infected and treated for 24 h with the two molecules by evaluating the IC50 values, which were found to be 0.128 mM and 0.077 mM for I-152 and I-152SdAc, respectively, markedly lower than CC50 values that were 1.89 mM and 0.7 mM for I-152 and I-152SdAc respectively (not shown), suggesting that the antiviral effect observed is not due to toxicity of the molecules.

3.3 | Thiol molecules increase intracellular thiol content and affect Spike protein domains folding/production in HEK293 cells

The mechanisms by which the thiol molecules could inhibit SARS-CoV-2 replication were explored in HEK293 cells stably expressing the RBD/S1(D614G) domains since both the biogenesis of CoV-2 viral proteins and the production of recombinant proteins in mammalian cells require an efficient host's secretory protein factory which is known to be sensible to redox shifts.[30,31]

Cells were treated for 24 h with different molecule concentrations and the amount of intracellular and secreted RBD was evaluated. Results shown in Figure 4A demonstrate that I-152 and I-152SdAc at 1 mM concentration were able to significantly reduce the amount of the secreted protein. A 40% reduction compared to control was also observed with 0.25 mM I-152, albeit not statistically significant. The decreased amount of secreted protein was paralleled by an intracellular accumulation of the protein only in the case of I-152SdAc (Figure 4B). As already demonstrated in other cell models,[32] analysis of the free thiol pools showed that within cells I-152 and I-152SdAc release high amounts of thiol species in the form of NAC, MEA, and cysteine and at the same time increase GSH concentration, thus creating a thiol-rich environment made of multiple thiol species which may interfere with oxidative protein folding (Figure 4C). On the other hand, C4-GSH-based redox change is mainly due to an increase in GSH (in the form of C4-GSH) and cysteine (Figure 4C). To shed light on the molecular mechanism affecting protein production/secretion, HEK293 cells expressing the S1 protein domain were treated with either I-152 or I-152SdAc, and the redox state of sulfhydryl S1 protein groups was assessed by thiol PEGylation and subsequent

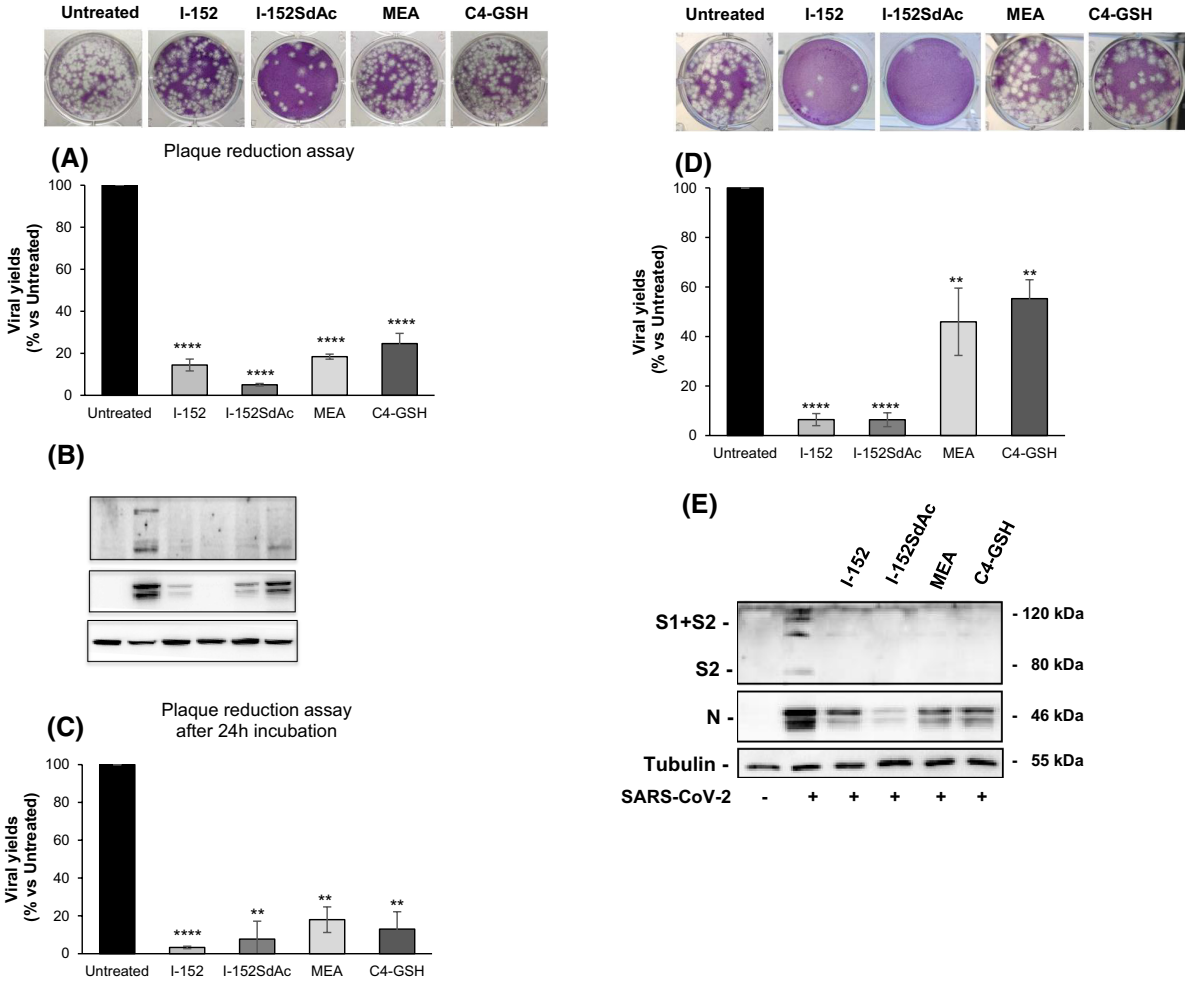

FIGURE 3 Inhibition of SARS-CoV-2 infectivity by thiol molecules in Vero E6 cells. Left: Inhibition of SARS-CoV-2 entry. (A) SARS-CoV-2 (0.01 m.o.i.) was incubated with I-152, I-152SdAc, and MEA (2 mM) or C4-GSH (20 mM) for 1 h at 37°C (thiol molecule+virus). Then, the mixtures were used to infect cells monolayer for 1 h at 37°C, and after the inoculum removal, plaque assay was performed. (B) Western immunoblotting analysis of Spike (S) and Nucleocapsid (N) protein levels in the cells uninfected or infected with the virus pre-incubated with the thiol molecules. Actin was stained as a loading control. Untreated virus suspension was used as a positive control. (C) Plaque assay performed in the cells infected with the supernatants derived from the cells previously infected with the mixture containing the thiol molecule+virus. Right: Inhibition of SARS-CoV-2 replication. (D) Cells were infected for 1 h at 37°C with SARS-CoV-2 (0.01 m.o.i.) and then treated with I-152, I-152SdAc and MEA (0.25 mM) or C4-GSH (10 mM) for 24 h. (E) Western immunoblotting analysis of Spike (S) and Nucleocapsid (N) proteins in the cells uninfected, infected either untreated or treated with thiol molecules. Tubulin was used as a loading control. Infected untreated cells were used as a positive control. Plaque number estimation was performed as described in Materials and methods. Data are obtained from at least 3 independent experiments, each performed in triplicate ($n = 9$), and are shown as mean ± standard deviation of the percentage of virus yields vs. the Untreated. ****$p < 10^{-4}$; ***$p < 10^{-3}$; **$p < 10^{-2}$.

western immunoblotting analysis with an anti S1 antibody (Figure 4D). As a reference, cells were incubated with reducing (DTT) and oxidant (diamide) agents to generate fully reduced and fully oxidized forms of the S1 subunit. In this assay, thiol groups undergo alkylation that shifts electrophoretic mobility to a higher molecular weight, whereas disulfide bonds remain without alkylation. Mal-PEG alkylation of a single sulfhydryl results in an apparent molecular mass shift of ~15 kDa as observed by SDS-PAGE.[33,34] These experiments demonstrated a dose-dependent switch from the oxidized to the reduced state of the S1 protein in cells treated with I-152 and I-152SdAc, thus highlighting the potential of these molecules and/or of their metabolites to directly/indirectly interfere with spike protein folding.

4 | DISCUSSION

Despite the multiple efforts to find reliable anti-CoV-2 therapies, no broad-spectrum antiviral drugs for combatting SARS-CoV-2 infection have been found to date. Thiol-based compounds, mainly anti-mucolytic compounds, have been found effective in preventing virus entry via

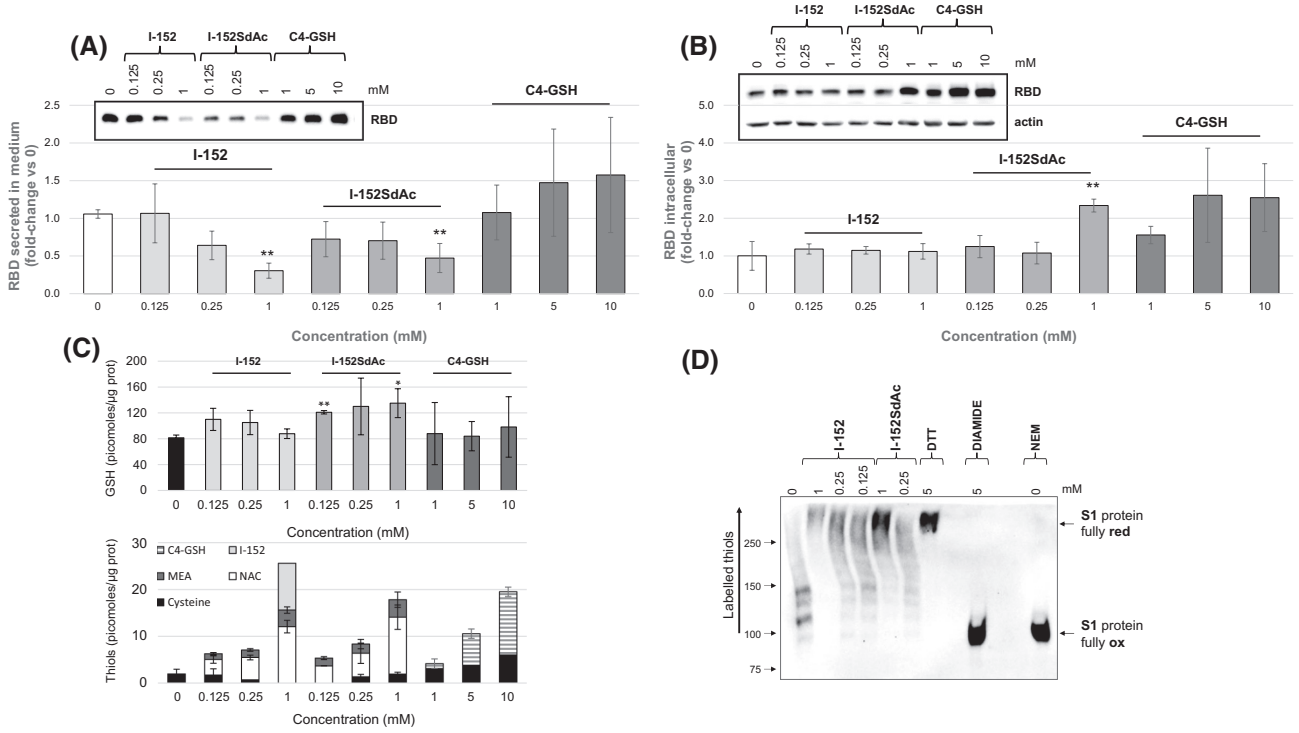

FIGURE 4 Modification of thiol content and folding/production of Spike protein domains by thiol molecules in HEK293 cells. Western immunoblotting analysis and quantification of secreted (A) and intracellular RBD protein (B) in RBD-expressing HEK293 cells. After 24 h treatment with the molecules, cell lysates (10 µg) and an aliquot of the culture medium (10 µl) were separated in SDS-PAGE and immunoblotted with an antibody against the His tag. Actin was stained as a loading control in lysates. Immunoreactive bands were quantified and the values were expressed as fold-change vs. untreated cells (0). Bars represent the mean ± SD from 3 independent experiments. (C) Thiol species in treated or untreated (0) cells. After 2 h-treatment with the thiol molecules, cells were washed and lysed; the lysate was then treated with precipitating solution and centrifuged. Thiol species and GSH levels were determined in the lysate supernatant by HPLC, while protein content was quantified spectrophotometrically in the lysate pellet. Quantification of thiol species was obtained by injection of standards of known concentrations and values were normalized on protein concentration. Data are obtained from at least 3 independent experiments. (D) Thiol redox state of S1 protein in HEK293 cells treated with different molecule concentrations as detected by thiol modification with Peg maleimide followed by western Immunoblotting analysis of cell lysates with an anti-spike protein antibody. Fully reduced and fully oxidized S1 were obtained from cells treated with the reducing agent DTT and the oxidizing compound diamide, respectively. The specificity of the assay was demonstrated by incubation of the cells with NEM prior to the pegylation procedure. On the left, the position of molecular weight standards (kDa) is indicated by arrows. $^{**}p < 10^{-2}$; $^{*}p < 5 \times 10^{-2}$ vs. 0.

disulfide bond reduction into RBD of the spike protein.[3–5] In line with this evidence, here, we demonstrate that synthetic LMW thiols I-152 and C4-GSH (monothiols) as well as I-152SdAc (dithiol) reduce disulfide bonds present in the RBD domain of SARS-CoV-2 spike protein and modify the RBD's disulfide linkage pattern thus inducing conformational changes that affect the binding of the protein to the ACE2 receptor. The interaction between RBD and ACE2 in the presence of the thiol molecules has been characterized by multiple assays. All the thiol molecules, although with different efficiencies, reduced all four disulfide bonds resulting in inhibition of the binding of the spike protein to ACE2 and virus entry, confirming the importance of disulfide integrity in the RBD of the SARS-CoV-2 spike protein for virus infectivity.[1–6] Among the monothiols, I-152 was the most potent, likely due to the different reactive thiolate populations at the working pH and/or the unfavorable Coulombic interactions (C4-GSH has a net charge of −2, and MEA preserves the cationic charge) near neutral pH.[35] Other reports have shown that thiol molecules, such as NAC and GSH,[25] impair RBD/ACE2 interaction but at higher concentrations, and some thiol-based chemical probes inhibit ACE2 binding and SARS-CoV-2 entry by breaking two disulfides at concentrations ranging from 3 to 30 mM.[5] In agreement with this investigation, the dithiol I-152SdAc was more effective than I-152 in RBD/ACE2 interaction tests and virucidal assays. Hence, I-152SdAc may represent a valid alternative to DTT that, although able to alter the spike architecture and prevent virus penetration, its use is hampered by toxicity.[36,37]

These thiol molecules, acting outside the cell, may inhibit SARS-CoV-2 infectivity both by reducing the disulfide bonds on the RBD domain and by altering the

thiol–disulfide balance that plays a key role in the binding of the spike glycoprotein onto the host cell receptor protein ACE2.[2] These results suggest that our molecules by targeting efficiently spike disulfides, impair ACE2/RBD interaction and virus entry. However, we can hypothesize that being membrane-permeant, these molecules could also block early viral events within the cell; thiol drugs have been demonstrated to react with cysteine residues on the protease of SARS-CoV-2 essential for viral replication.[38]

To our knowledge, what has not yet been demonstrated is that cell-penetrating thiol-based drugs could interfere with one of the late steps involved in virus replication. In particular, SARS-CoV infection modulates the unfolded protein response (UPR), characterized by the transcriptional activation of ER chaperons, necessary for the folding as well as the processing of viral proteins and particularly sensitive to redox changes.[39,40] The thiol molecules studied fine-tune the intracellular thiol/disulfide redox pools in different ways that could explain the different antiviral efficiencies found. C4-GSH can mainly increase intracellular GSH content.[41] By contrast, I-152 provides, once hydrolysis occurs, other thiol species beyond GSH, i.e. NAC, MEA, cysteine (Figure 4C), and, by its known intermolecular process of transposition, the corresponding fully acetylated derivative, and the dithiol I-152SdAc.[18,21,32] Furthermore, I-152 was found to induce the antioxidant response through activation of the transcription factor Nrf2.[32] All these evidences support the hypothesis that modulation of the redox state through the thiol molecules can affect the oxidative folding of disulfide-rich viral proteins leading to impairment of mature virions production. Indeed, I-152SdAc and I-152 interfere with the oxidative folding/secretion of RBD/S1 in HEK 293 cells. However, only I-152SdAc induced an intracellular RBD accumulation, as if in I-152-treated cells the unfolded/misfolded protein may be recognized, retrotranslocated, ubiquitinated, and finally degraded by the proteasome,[42] but this aspect needs to be further investigated. Concerning this matter, we may exclude an overall reduction in protein expression levels since intracellular RBD levels in treated cells are not significantly different from control cells (Figure 4B). Moreover, we have previously demonstrated that I-152 treatment of RAW 264.7 cells with concentrations up to 1 mM induces Nrf2 activation, an effect dependent on de novo protein synthesis, and targets gene expression both at the mRNA and protein levels up to 24 h, demonstrating that the molecule does not significantly affect overall protein expression.[32] Although C4-GSH did not affect RBD secretion in the context of the stably transfected HEK 293 cells, it blocked SARS-CoV-2 replication by about 50% while viral inhibition by I-152SdAc and I-152 was superior to 90%. The similar intracellular effects of I-152 and I-152SdAc could be due to their similar metabolism inside the host cell. While the higher intracellular antiviral activity of I-152 compared to the other monothiols (MEA and C4-GSH) may be due just to the thiol-based redox switch induced by the thiol species delivered by I-152. Indeed antiviral concentration range of C4-GSH is much higher, i.e., 10–20 mM, which are the doses that had been previously demonstrated to contrast influenza virus infection even more sharply.[19] This finding suggests that glutathione-mediated redox switch may be not sufficient to hamper so effectively SARS-CoV-2 infection as the influenza one and that redox state may play an even more important role in controlling SARS-CoV-2 replication than other respiratory viruses.[12,43,44] Since I-152 and I-152SdAc can be converted by enzymatic action into cysteine and cysteamine (MEA), both of them could be a valid alternative to MEA; in fact, although this molecule has demonstrated anti-SARS-CoV-2 activity,[3,27,45] the clinical use is limited by its strong hygroscopicity, poor pharmacokinetic profile and tendency to undergo oxidation to disulfide cystamine.[28] Overall, these data demonstrate that our synthetic thiol compounds could inhibit SARS-CoV-2 infectivity by two mechanisms: by inhibiting virus entry and by interfering with the production of mature virions. In conclusion, these molecules are good models for the development of new broad-spectrum drugs that on the one hand target the first step in SARS-CoV-2 infection, and on the other hand, host factors useful for viral replication so reducing the possibility of resistance development and potentially acting against viral variants.

AUTHOR CONTRIBUTIONS

Alessandra Fraternale, Lucia Nencioni, and Rita Crinelli conceived and designed the research; Alessandra Fraternale, Marta De Angelis, Riccardo De Santis, Donatella Amatore, Sofia Masini, Francesca Monittola, Michele Menotta, Federica Biancucci, Francesca Bartoccini, Michele Retini, Valentina Fiori, Raoul Fioravanti, Fabio Magurano, Laura Chiarantini, Lucia Nencioni, and Rita Crinelli performed the research and acquired the data; Alessandra Fraternale, Marta De Angelis, Riccardo De Santis, Donatella Amatore, Sofia Masini, Michele Menotta, Raoul Fioravanti, Fabio Magurano, Anna T. Palamara, Lucia Nencioni, Mauro Magnani, and Rita Crinelli analyzed and interpreted the data. All authors were involved in drafting and revising the manuscript.

ACKNOWLEDGMENTS

This work was supported by: University of Urbino grants (DISB_CRINELLI_PROG_SIC_ALIMENTARE); Sapienza University grants RM120172B6D0AD25 and RP12117A62FD5A1A (LN); Italian Ministry for University and Research: MUR PRIN 2020KSY3KL (ATP) 2020AEX4TA (GP) grants.

DISCLOSURES

The authors declare no conflict of interest.

DATA AVAILABILITY STATEMENT

The data that support the findings of this study are available on request from the corresponding author.

ORCID

Alessandra Fraternale https://orcid.org/0000-0002-7893-3842
Fabio Magurano https://orcid.org/0000-0002-0394-7043
Lucia Nencioni https://orcid.org/0000-0003-4427-4823

REFERENCES

1. Hati S, Bhattacharyya S. Impact of thiol–disulfide balance on the binding of Covid-19 spike protein with angiotensin-converting enzyme 2 receptor. *ACS Omega*. 2020;5:16292-16298.
2. Giustarini D, Santucci A, Bartolini D, Galli F, Rossi R. The age-dependent decline of the extracellular thiol-disulfide balance and its role in SARS-CoV-2 infection. *Redox Biol*. 2021;41:101902.
3. Khanna K, Raymond WW, Jin J, et al. Exploring antiviral and anti-inflammatory effects of thiol drugs in COVID-19. *Am J Physiol Lung Cell Mol Physiol*. 2022;323:L372-L389.
4. Manček-Keber M, Hafner-Bratkovič I, Lainšček D. Disruption of disulfides within RBD of SARS-CoV-2 spike protein prevents fusion and represents a target for viral entry inhibition by registered drugs. *FASEB J*. 2021;35:e21651.
5. Shi Y, Zeida A, Edwards CE, et al. Thiol-based chemical probes exhibit antiviral activity against SARS-CoV-2 via allosteric disulfide disruption in the spike glycoprotein. *Proc Natl Acad Sci U S A*. 2022;119:e2120419119.
6. Grishin AM, Dolgova NV, Landreth S, et al. Disulfide bonds play a critical role in the structure and function of the receptor-binding domain of the SARS-CoV-2 spike antigen. *J Mol Biol*. 2021;434:167357.
7. Singh J, Dhindsa RS, Misra V, Singh B. SARS-CoV2 infectivity is potentially modulated by host redox status. *Comput Struct Biotechnol J*. 2020;18:3705-3711.
8. Yadav R, Chaudhary JK, Jain N, et al. Role of structural and non-structural proteins and therapeutic targets of SARS-CoV-2 for COVID-19. *Cell*. 2021;10:821.
9. Hwang C, Sinskey AJ, Lodish HF. Oxidized redox state of glutathione in the endoplasmic reticulum. *Science*. 1992;257:1496-1502.
10. Fernandes IG, de Brito CA, Dos Reis VMS, Sato MN, Pereira NZ. SARS-CoV-2 and other respiratory viruses: what does oxidative stress have to do with it? *Oxid Med Cell Longev*. 2020;2020:8844280.
11. Camini FC, da Silva Caetano CC, Almeida LT, de Brito Magalhães CL. Implications of oxidative stress on viral pathogenesis. *Arch Virol*. 2017;162:907-917.
12. Bartolini D, Stabile AM, Bastianelli S, et al. SARS-CoV2 infection impairs the metabolism and redox function of cellular glutathione. *Redox Biol*. 2021;45:102041.
13. Oiry J, Mialocq P, Puy JY, et al. Synthesis and biological evaluation in human monocyte-derived macrophages of N-(N-acetyl-l-cysteinyl)-S-acetylcysteamine analogues with potent antioxidant and anti-HIV activities. *J Med Chem*. 2004;47:1789-1795.
14. Fraternale A, Zara C, Di Mambro T, et al. I-152, a supplier of N-acetyl-cysteine and cysteamine, inhibits immunoglobulin secretion and plasma cell maturation in LP-BM5 murine leukemia retrovirus-infected mice by affecting the unfolded protein response. *Biochim Biophys Acta Mol Basis Dis*. 2020;1866:165922.
15. Amatore D, Celestino I, Brundu S, et al. Glutathione increase by the n-butanoyl glutathione derivative (GSH-C4) inhibits viral replication and induces a predominant Th1 immune profile in old mice infected with influenza virus. *FASEB Bioadv*. 2019;1:296-305.
16. Nencioni L, Sgarbanti R, Amatore D, et al. Intracellular redox signaling as therapeutic target for novel antiviral strategy. *Curr Pharm Des*. 2011;17:3898-3904.
17. Palamara AT, Brandi G, Rossi L, et al. New synthetic glutathione derivatives with increased antiviral activities. *Antivir Chem Chemother*. 2004;15:77-85.
18. Crinelli R, Zara C, Smietana M, Retini M, Magnani M, Fraternale A. Boosting GSH using the Co-drug approach: I-152, a conjugate of N-acetyl-cysteine and β-mercaptoethylamine. *Nutrients*. 2019;11:1291.
19. Sgarbanti R, Nencioni L, Amatore D, et al. Redox regulation of the influenza hemagglutinin maturation process: a new cell-mediated strategy for anti-influenza therapy. *Antioxid Redox Signal*. 2011;15:593-606.
20. Bartoccini F, Mari M, Retini M, Fraternale A, Piersanti G. Large-scale preparation of N-Butanoyl-l-glutathione (C4-GSH). *Org Process Res Dev*. 2019;23:2069-2073.
21. Bartoccini F, Retini M, Crinelli R, Menotta M, Fraternale A, Piersanti G. Dithiol based on L-cysteine and cysteamine as a disulfide-reducing agent. *J Org Chem*. 2022;87:10073-10079.
22. Lan J, Ge J, Yu J, et al. Structure of the SARS-CoV-2 spike receptor-binding domain bound to the ACE2 receptor. *Nature*. 2020;581:215-220.
23. Fraternale A, Crinelli R, Casabianca A, et al. Molecules altering the intracellular thiol content modulate NF-kB and STAT-1/IRF-1 signalling pathways and IL-12 p40 and IL-27 p28 production in murine macrophages. *PLoS One*. 2013;8:e57866.
24. Brundu S, Nencioni L, Celestino I, et al. Validation of a reversed-phase high performance liquid chromatography method for the simultaneous analysis of cysteine and reduced glutathione in mouse organs. *Oxid Med Cell Longev*. 2016;2016:1746985.
25. Murae M, Shimizu Y, Yamamot Y, et al. The function of SARS-CoV-2 spike protein is impaired by disulfide-bond disruption with mutation at cysteine-488 and by thiol-reactive N-acetylcysteine and glutathione. *Biochem Biophys Res Commun*. 2022;597:30-36.
26. Braakman I, Lamriben L, van Zadelhoff G, Hebert DN. Analysis of disulfide bond formation. *Curr Protoc Protein Sci*. 2017;90:14.1.1-14.1.21.
27. Thoene J, Gavin RF, Towne A, et al. In vitro activity of cysteamine against SARS-CoV-2 variants. *Mol Genet Metab*. 2022;137:192-200.
28. Atallah C, Charcosset C, Greige-Gerges H. Challenges for cysteamine stabilization, quantification, and biological effects improvement. *J Pharm Anal*. 2020;10:499-516.

29. Ariceta G, Giordano V, Santos F. Effects of long-term cysteamine treatment in patients with cystinosis. *Pediatr Nephrol*. 2019;34:571-578.
30. Sicari D, Chatziioannou A, Koutsandreas T, Sitia R, Chevet E. Role of the early secretory pathway in SARS-CoV-2 infection. *J Cell Biol*. 2020;219:e202006005.
31. Gutierrez JM, Feizi A, Li S, et al. Genome-scale reconstructions of the mammalian secretory pathway predict metabolic costs and limitations of protein secretion. *Nat Commun*. 2020;11:68.
32. Crinelli R, Zara C, Galluzzi L, et al. Activation of NRF2 and ATF4 signaling by the pro-glutathione molecule I-152, a Co-drug of N-acetyl-cysteine and cysteamine. *Antioxidants (Basel)*. 2021;10:175.
33. Wilkinson B, Xiao R, Gilbert HF. A structural disulfide of yeast protein-disulfide isomerase destabilizes the active site disulfide of the N-terminal thioredoxin domain. *J Biol Chem*. 2005;280:11483-11487.
34. Fass D, Thorpe C. Chemistry and enzymology of disulfide cross-linking in proteins. *Chem Rev*. 2018;118:1169-1198.
35. Nagy P. Kinetics and mechanisms of thiol-disulfide exchange covering direct substitution and thiol oxidation-mediated pathways. *Antioxid Redox Signal*. 2013;18:1623-1641.
36. Held KD, Biaglow JE. Mechanisms for the oxygen radical-mediated toxicity of various thiol-containing compounds in cultured mammalian cells. *Radiat Res*. 1994;139:15-23.
37. Wang Y, Misto M, Yang J, Gehring N, Yu X, Moussian B. Toxicity of dithiothreitol (DTT) to drosophila melanogaster. *Toxicol Rep*. 2021;8:124-130.
38. Lobo-Galo N, Terrazas-López M, Martínez-Martínez A, Díaz-Sánchez ÁG. FDA-approved thiol-reacting drugs that potentially bind into the SARS-CoV-2 main protease, essential for viral replication. *J Biomol Struct Dyn*. 2021;39:3419-3427.
39. Chan CP, Siu KL, Chin KT, Yuen KY, Zheng B, Jin DY. Modulation of the unfolded protein response by the severe acute respiratory syndrome coronavirus spike protein. *J Virol*. 2006;80:9279-9287.
40. Echavarría-Consuegra L, Cook GM, Busnadiego I, et al. Manipulation of the unfolded protein response: a pharmacological strategy against coronavirus infection. *PLoS Pathog*. 2021;17:e1009644.
41. Fraternale A, Zara C, De Angelis M, et al. Intracellular redox-modulated pathways as targets for effective approaches in the treatment of viral infection. *Int J Mol Sci*. 2021;22:3603.
42. Ninagawa S, George G, Mori K. Mechanisms of productive folding and endoplasmic reticulum-associated degradation of glycoproteins and non-glycoproteins. *Biochim Biophys Acta Gen Subj*. 2021;1865:129812.
43. Khomich OA, Kochetkov SN, Bartosch B, Ivanov AV. Redox biology of respiratory viral infections. *Viruses*. 2018;10:E392.
44. Bellanti F, Lo Buglio A, Vendemiale G. Redox homeostasis and immune alterations in coronavirus disease-19. *Biology (Basel)*. 2022;11:159.
45. Alonzi T, Aiello A, Repele F, et al. Cysteamine exerts in vitro antiviral activity against the SARS-CoV-2 Delta and Omicron variants. *Cell Death Discov*. 2022;8:288.

SUPPORTING INFORMATION

Additional supporting information can be found online in the Supporting Information section at the end of this article.

How to cite this article: Fraternale A, De Angelis M, De Santis R, et al. Targeting SARS-CoV-2 by synthetic dual-acting thiol compounds that inhibit Spike/ACE2 interaction and viral protein production. *The FASEB Journal*. 2023;37:e22741. doi:10.1096/fj.202201157RR